Table of contents

Volume 367

2018

◂ Previous issue   Next issue ▸

The 5th International Conference on Advanced Materials Sciences and Technology (ICAMST 2017) 19–20 September 2017, Makassar, Indonesia

Accepted papers received: 16 May 2018

Published online: 12 June 2018

Open all abstracts

Preface

OPEN ACCESS 011001

The 5th International Conference on Advanced Materials Sciences and Technology (ICAMST 2017)

+ Open abstract   View article   PDF

OPEN ACCESS 011002

The List of Committee ICAMST 2017

+ Open abstract   View article   PDF

OPEN ACCESS 011003

List of Participant ICAMST 2017

+ Open abstract   View article   PDF

OPEN ACCESS 011004

Photographs

+ Open abstract   View article   PDF

OPEN ACCESS 011005

Peer review statement

+ Open abstract   View article   PDF

Papers

OPEN ACCESS 012001

OPEN ACCESS 012037

Influence of Annealing Time Variation on Crystal Structure and Morphology of Oxide Material $Nd_{1.2}FeO_3$ by Solid-State Reaction Method

E. H. Sujiono, A.C. M. Said, M. Y. Dahlan, R. A. Imran and S. Samnur

+ Open abstract   View article   PDF

OPEN ACCESS 012038

Porous Fe_2O_3 Microspheres as Anode for Lithium-Ion Batteries

L. Noerochim, M. A. T. Indra, H. Purwaningsih and A. Subhan

+ Open abstract   View article   PDF

OPEN ACCESS 012039

Analysis of Porosity Defects in Aluminum as Part Handle Motor Vehicle Lever Processed by High-pressure Die Casting

L. Anggraini and Sugeng

+ Open abstract   View article   PDF

OPEN ACCESS 012040

Synthesis and Characterization of Barium-Hexaferrite-Based Nanocomposite on X-Band Microwave

Y. E. Gunanto, M. P. Izaak, S. S. Silaban and W. A. Adi

+ Open abstract   View article   PDF

OPEN ACCESS 012041

Semiconductor Ceramic $Mn_{0.5}Fe_{1.5}O_3$-Fe_2O_3 from Natural Minerals as Ethanol Gas Sensors

H. Aliah, D. G. Syarif, R. N. Iman, A. Sawitri, M Sanjaya WS, M. Nurul Subkhi and P. Pitriana

+ Open abstract   View article   PDF

OPEN ACCESS 012042

The Effects of Calcination Temperatures on Crystal Structures and Morphologies of $Nd_{1.2}FeO_3$ Synthesized by Solid-State Reaction

E. H. Sujiono, M. Y. Dahlan, R. A. Imran, A.C. M. Said and S. Samnur

+ Open abstract   View article   PDF

OPEN ACCESS 012043

Synthesis and Characterization of Monodisperse Core-shell Lanthanide Upconversion Nanoparticles $NaYF_4$: Yb,Tm/SiO_2

R. V. Manurung, G. Wiranto and I. D. P. Hermida

+ Open abstract   View article   PDF

OPEN ACCESS 012044

IOP Conference Series: Materials Science and Engineering

The Effects of Calcination Temperatures on Crystal Structures and Morphologies of $Nd_{1.2}FeO_3$ Synthesized by Solid-State Reaction

To cite this article: E. H. Sujiono *et al* 2018 *IOP Conf. Ser.: Mater. Sci. Eng.* **367** 012042

The Effects of Calcination Temperatures on Crystal Structures and Morphologies of $Nd_{1.2}FeO_3$ Synthesized by Solid-State Reaction

E. H. Sujiono[1], M. Y. Dahlan[1], R. A. Imran[1], A.C. M. Said[1], and S. Samnur[1]

[1]Laboratory of Materials Physics Department of Physics, Universitas Negeri Makassar, Makassar 90224, Indonesia

E-mailr: e.h.sujiono@unm.ac.id

Abstract. $NdFeO_3$ is one of the oxide alloys that can be used as a raw material for gas sensor. The $NdFeO_3$ have been synthesized using solid state reaction method by varying calcination temperatures of 750ºC, 850ºC, and 950ºC for 6 h. All of the $Nd_{1.2}FeO_3$ samples were characterized using scanning electron microscope (SEM) and x-ray diffraction (XRD) to identify their morphologies and phases. The results show that all of the samples formed major phase is $NdFeO_3$ and minor phase of Nd_2O_3 and have homogenous morphology with estimating grain size is 0,2 µm for all samples. The value of FWHM and the crystal size of $Nd_{1.2}FeO_3$ was obtained for each sample is 0.22º and 372 nm. The orthorhombic phase with a dominant peak at *hkl* (121) is an indication that material has potential application as a gas sensor.

Keywords. Crystal structure, morphology, calcination, $NdFeO_3$, and solid state method.

1. Introduction

As increasing awareness of environmental issues and the development of industrial rapidly that affects pollutant gas emissions makes the demand for sensors increases. The active material in the gas sensor can be metal, metal oxide, composite polymer and conductive polymer but now also developed active material on gas sensor derived from oxide alloy material. In recent years, $NdFeO_3$ perovskite structure has been investigated its usefulness in a wide variety of applications such as in oxide fuel cells [1], gas sensors [2], the photocatalysis and catalytic converter [3]. $NdFeO_3$ has a perovskite-type orthorhombic structure [4]. The preparation of $NdFeO_3$ has been successfully investigated by many methods, such as combustion [5], hydrothermal [6], sol-gel citrate method [7], precipitation [8], sonication assisted precipitation [9], and solid state reaction [10] are used. Solid state reaction is the most widely used for the synthesis of inorganic materials because it is easy and inexpensive by involving the heating components at a high temperature for a relatively long period. We have experiences in fabrication of such an oxide material, e.g., YBa2Cu3Oy, NdBaCuO (off-stoichiometric), and $NdFe_xBa_{2-x}Cu_3O_y$, the results have reported [11-13].

In this article, we reported our current results in the development of $Nd_{1.2}FeO_3$ oxide alloy material as one potential candidate for sensor application. $Nd_{1.2}FeO_3$ oxide have been synthesized using solid-state reaction method with two stages of heat treatment process and varying the calcination temperature. Characterization of material has been done by X-ray Diffraction (XRD) and Scanning Electron Microscope (SEM).

2. Materials and methods

$Nd_{1.2}FeO_3$ oxide alloy has been synthesized using solid-state reaction method [14]. The raw material Nd_2O_3 99.99 % (Strem Chemicals) and Fe_2O_3 99.99 % (Sigma Aldrich) were mixed and grinded together for 3 h then calcined for 6 h at temperature 700 ºC. The mixed powder then grinded for 5 h then sintered for 6 h at temperature 950 ºC. The synthesis process and the heating are then repeated to obtain a better sample homogeneity [15]. The mixed powder was grinded for 3 h and calcined at temperature 750 ºC, this process was repeated for temperature 850 ºC and 950 ºC. All of the powders were grinded for 5 h and sintered at temperature 950 ºC for 6 h.

$Nd_{1.2}FeO_3$ powder characterized by X-ray diffractometer [Rigaku Mini Flex II, 2θ = 20º – 65º (CuKα, λ = 0.154 nm)] to determine the crystal structure which includes the value of FWHM (Full Width at Half Maximum) and peak height. The analysis of surface morphology and elemental of the powder were investigated using Scanning Electron Microscope and Energy Dispersive Spectroscopy (SEM-EDS) [Tescan Vega3SB] with a magnification of 5000 times.

3. Results and discussion

XRD diffraction patterns of oxide material $Nd_{1.2}FeO_3$ powder were synthesized by using the solid-state reaction method with variations of calcination temperature at temperatures of 750 ºC, 850 ºC and 950 ºC are shown in Figure 1.

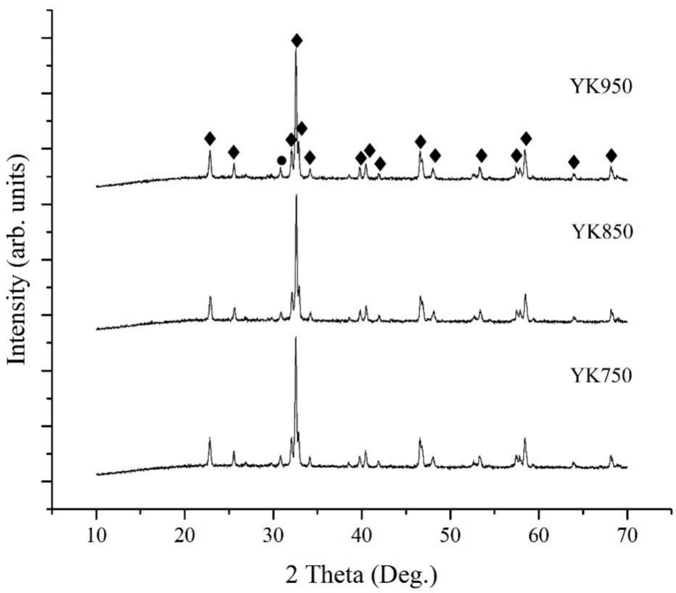

Figure 1. XRD patterns of $Nd_{1.2}FeO_3$ as variation of calcination temperatures (♦ = $NdFeO_3$, • = Nd_2O_3)

Figure 1 shows the peak of $NdFeO_3$ and Nd_2O_3 phase have been identified based on data adjustment using the Match! Software. This crystallographic curve shows that Nd_2O_3 and Fe_2O_3 raw materials have been formed of the new phase of $NdFeO_3$ which crystallizes in the orthorhombic system. The existence of minor phase formation of Nd_2O_3 is an indication that $Nd_{1.2}FeO_3$ raw material does not produce perfect phase. The reaction of imperfection is suspected due to the adjustment of calcination temperature and the heating time is less than optimal. On the other hand, Niu Xinshu et al.

also successfully synthesized $NdFeO_3$ with a temperature of 950 ºC [16] and Yabin Wang et al. with a temperature of 1000 ºC [17]. The results are similar to the current study with an indication of the dominant phase formation of $NdFeO_3$ located at $2\theta = 32.56^{\circ}$ corresponding to the *hkl* value (121). The dominant phase intensity *hkl* (121) increases when the heating temperature is increased [18].

The crystal size can be estimated by using Debye-Scherer equation as described in Equation 1:

$$D = \frac{0.9\lambda}{\beta \cos\theta} \quad (1)$$

Where λ is the wavelength of the radiation Cu Kα (λ = 0.154 nm), θ is the angle Bragg (º), and β = FWHM at the peak of *hkl* (121) is association 2θ of 32.56º [19]. The calculation results of crystal size and FWHM can be seen in Table 1.

Table 1. Data Position (2θ), intensity, FWHM value and crystal size of $Nd_{1.2}FeO_3$ phase

Samples	2θ (º)	Intensity (Counts)	FWHM (º)	Crystal Size (nm)
YK 750	32.56	13063.33	0.22	372.17 ± 0.02
YK 850	32.56	12686.67	0.22	372.22 ± 0.02
YK 950	32.56	13050.00	0.22	372.17 ± 0.02

Based on the Table 1, it can be seen that the FWHM values for each sample are same in order of 0.22º. Full-width at half maximum (FWHM) is still an effective method to confirm the quality of crystal structure [17]. FWHM value was influenced by the intensity of each crystal plane. The higher intensity is resulting in smaller FWHM value which indicating the good crystallinity of the samples.

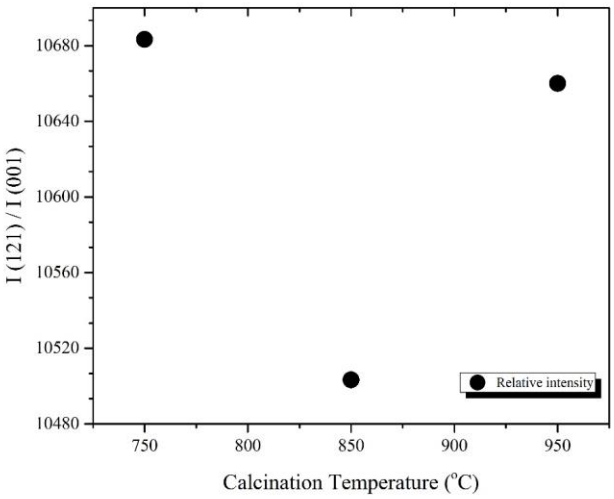

Figure 2. The comparison of the relative peak intensity of $Nd_{1.2}FeO_3$ samples with the variations of calcination temperature

Figure 2 shows the calculation result of relative intensities curve for each variation of calcination temperature. These results found that the variation of calcination temperature did not a significant change of crystal size of the sample. In fact, the existences of the atom due to the Nd_2O_3 phase will reduce the diffraction intensity of each sample. Sample with calcination temperature of 850 ºC at peak *hkl*(121) is more dominant than other peaks. Thus, the $Nd_{1.2}FeO_3$ oxide material with the parameters process as has explained above will be useful for the application as gas sensors as has been reported elsewhere [2, 9, 16].

The morphology, structure and particle size of samples $Nd_{1.2}FeO_3$ as a variation of calcination temperature were investigated by SEM. Figure 3 shows the SEM micrograph of the samples.

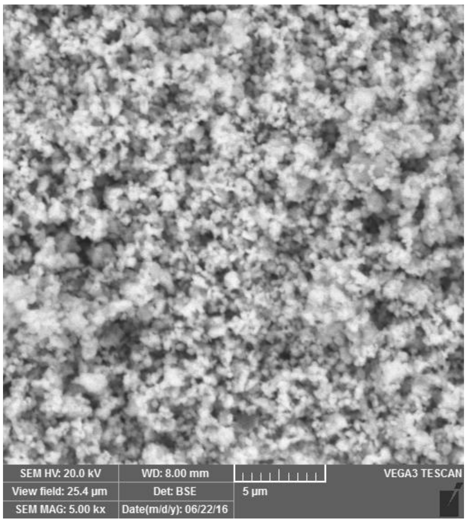

(a)

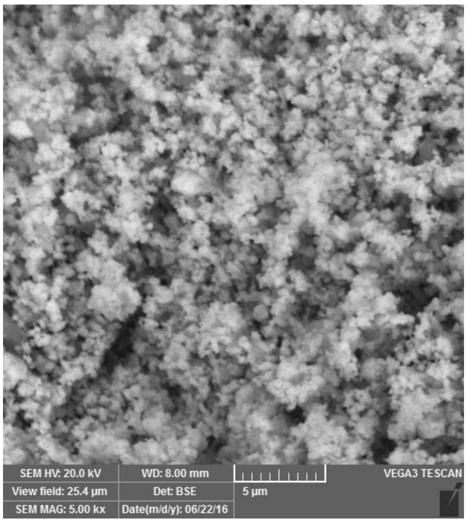

(b)

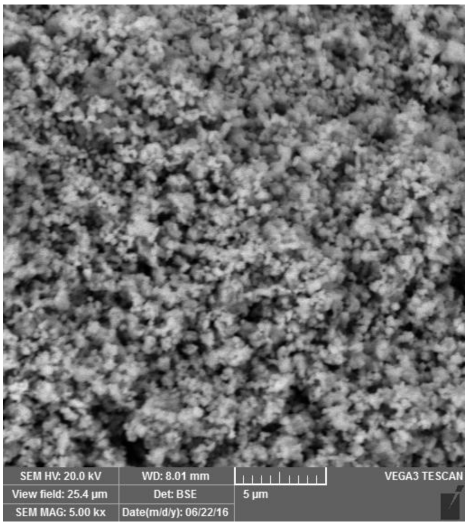

(c)

Figure 3. Morphology of sample $Nd_{1.2}FeO_3$ as a variation of calcination temperature (a) YK750, (b) YK850 and (c) YK950, respectively

Table 2. Data composition element of $Nd_{1.2}FeO_3$ samples using EDS

Element	Norm. C [wt%]			Error (3 Sigma) [wt%]		
	YK750	YK850	YK950	YK750	YK850	YK950
Sodium	1.30	1.04	1.54	0.40	0.35	0.42
Magnesium	0.61	0.31	0.76	0.22	0.16	0.24
Aluminium	0.34	0.39	0.56	0.16	0.17	0.19
Silicon	0.17	0.46	-	0.12	0.16	-
Oxygen	17.20	17.33	17.19	6.63	6.83	5.77
Potassium	0.12	0.10	0.04	0.10	0.10	0.09
Titanium	0.17	0.21	0.14	0.11	0.12	0.11
Iron	20.38	20.16	20.09	1.74	1.75	1.49
Copper	0.35	0.15	0.74	0.17	0.13	0.22

Neodymium	59.36	59.83	58.94	4.76	4.91	4.02
Total :	100	100	100			

In Figure 3, it can be observed that all samples have high homogeneity indicated by the morphology of the sample forming small uniform granules, while the estimated grain size of each sample is 0.2 μm. This powder has high porosity, and this is one of the benefits to improve the characteristics of the $NdFeO_3$ oxide alloy material as a gas sensor application, as disclosed by Ho et al. [2].

The EDS results showed that $Nd_{1.2}FeO_3$ samples of YK750, YK850, and YK950 has contained Fe (20.38 wt%), Fe (20.16 wt%), Fe (20.09 wt%) and Nd (59.36 wt%), Nd (59.83 wt%), Nd (58.94 wt%), respectively and also contains a minor phase as shown in Table 2. It can be seen; there is no significant effect on the constituent elements of each sample. That existing of minor phase as indication due to the sample holder preparation process.

4. Conclusions

The $Nd_{1.2}FeO_3$ powders as a variation of calcination temperature of 750 ºC, 850 ºC, and 950 ºC have been successfully synthesized using solid state reaction method. The results of X-ray diffraction analysis showed $NdFeO_3$ and Nd_2O_3 phase, in which the crystal structure of the phase $NdFe_{1.2}O_3$ is orthorhombic to the space group Pnma. Variation of calcination temperature higher than 700 ºC did not the significant influence of diffraction intensity, FWHM, and crystallite size.

All of the samples have homogeneous morphology and high porosity with an estimated grain size of 0.2 μm. This study has been obtained compound $NdFe_{1.2}O_3$ oxide alloy with the dominant peak of *hkl* (121) which indicated that the sample is a good candidate for a gas sensor material as has been reported elsewhere.

Acknowledgements

This research was funded by Directorate Research and Community Services, Directorate General of Research and Development, Ministry of Research, Technology, and Higher Education, Republic of Indonesia, under research scheme of *Hibah Kompetensi* fiscal year 2017.

References

[1] Chen T *et al* 2012 $NdFeO_3$ as anode material for S/O_2 solid oxide fuel cells *Journal of Rare Earths* **30** 1138 – 1141
[2] Ho T G *et al* 2011 *Advanced in Natural Science: Nanoscience and Nanotechnology* **2** 015012 – 15021
[3] Niu X, Li H, and Liu G 2005 Preparation, characterization and photocatalytic properties of REFeO3 (RE= Sm, Eu, Gd) *Journal of Molecular Catalysis A: Chemical* **232** 89 – 93
[4] Chen L *et al* 2012 The role of 4f-electron on spin reorientation transition of $NdFeO_3$: A first principle study *Journal of Applied Physics* **111** 103905
[5] Wu A *et al* 2009 Preparation of $ReFeO_3$ nanocrystalline powders by auto-combustion of citric acid gel *Asia-Pacific Journal of Chemical Engineering* **45** 518 – 521
[6] Zheng W *et al* 2000 Hydrothermal synthesis of $LaFeO_3$ under carbonate-containing medium *Materials Letters* **43** 19 – 22
[7] Cui H, Zayat M, and Levy D 2006 Epoxide assisted sol–gel synthesis of perovskite-type $LaMxFe_{1-x}O_3$ (M= Ni, Co) nanoparticles *Journal of Non-Crystalline Solids* **352** 3035 – 3040
[8] Khorasani-Motlagh M et al 2013 *International Journal of Nanoscience and Nanotechnology* **9** 17 – 14
[9] Singh S *et al* 2013 Fabrication of nanobeads structured perovskite type neodymium iron oxide film: Its structural, optical, electrical and LPG sensing investigations *Sensors and Actuators B: Chemical* **177** 730 – 739
[10] Smart L and Moore E 2005 *Solid State Chemistry* (CRC Press, Boca Raton)
[11] Sujiono E H *et al* 2001 Crystal Structure and Morphology Analysis of $Nd_{1+x}Ba_{2-x}Cu_3O_7$ Oxide

Alloy Surface Developed by Solid State Reaction Method *Physica Status Solidi (A) Applied Research* **187** 471 – 479

[12] Sujiono E H, Arifin P, and Barmawi M. 2002 $YBa_2Cu_3O_{7-\delta}$ thin films deposited by a vertical MOCVD reactor *Materials Chemistry and Physics* **73** 47 – 50

[13] Sujiono E H 2017 Paduan oksida logam Nd1(Fe)XBa$_2$-XCu$_3$OY dan metode pembuatannya ID Patent No. P00200800471

[14] Zharvan V et al 2017 The Effect of Molar Ratio on Crystal Structure and Morphology of $Nd_{1+X}FeO_3$ (X=0.1, 0.2, and 0.3) Oxide Alloy Material Synthesized by Solid State Reaction Method *IOP Conference: Materials Science and Engineering* **202** 012072

[15] Mir S A, Ikram M, and Asokan K 2014 *Optik - International Journal for Light and Electron Optics* **125** 6903 – 6908

[16] Niu X *et al* 2003 *Journal of Rare Earths* **21** 630

[17] Wang Y *et al* 2010 Growth rate dependence of the $NdFeO_3$ single crystal grown by float-zone technique *Journal of Crystal Growth* **318** 927 – 931

[18] Aono H *et al* 1998 Characterizations of $NdFe_{0.5}Co_{0.5}O_3$ Trimetallic Oxide Prepared by Thermal Decomposition of Heteronuclear Complex , $Nd[Fe_{0.5}Co_{0.5}(CN)_6]_4H_2O$ *Journal Ceramic Society of Japan* **106** 10

[19] Chanda S *et al* 2013 Raman spectroscopy and dielectric properties of nanoceramic $NdFeO_3$ *Materials Research Bulletin* **48** 1688 – 1693